

Universal Parity Quantum Computing

Michael Fellner,^{1,2} Anette Messinger,² Kilian Ender,^{1,2} and Wolfgang Lechner^{1,2}

¹*Institute for Theoretical Physics, University of Innsbruck, A-6020 Innsbruck, Austria*

²*Parity Quantum Computing GmbH, A-6020 Innsbruck, Austria*

(Dated: May 20, 2022)

We propose a universal gate set for quantum computing with all-to-all connectivity and intrinsic robustness to bit-flip errors based on the parity encoding. We show that logical CPhase gates and R_z rotations can be implemented in the parity encoding with single-qubit operations. Together with logical R_x rotations, implemented via nearest-neighbor CNOT gates and an R_x rotation, these form a universal gate set. As the CPhase gate requires only single qubit rotations, the proposed scheme has advantages for several cornerstone quantum algorithms, e.g. the Quantum Fourier Transform. We present a method to switch between different encoding variants via partial on-the-fly encoding and decoding.

Designing quantum computers [1–18] and quantum algorithms [19–27] is a current grand challenge in science and engineering, motivated by the prospect of solving certain problems exponentially faster than any classical computer [22]. However, the fundamental rules of quantum mechanics that make this new paradigm possible also impose fundamental restrictions. In contrast to bits, quantum bits cannot be copied, only exchanged or *swapped*, which is known as the no-cloning theorem. Thus, quantum computers will not be able to follow the von Neumann architecture [28] with separated memory and computational unit. As the quantum CPU serves as memory and computational unit at the same time, connectivity between any quantum bits on the chip is required. In current standard approaches to gate-based quantum computers, these long-range interactions are implemented either as physical interactions, which limits scalability, or quantum information is moved on the chip via SWAP sequences, which requires a large overhead in gates.

In this work, we propose a novel universal quantum computing approach based on the LHZ architecture [29]. In this parity-based paradigm, each physical qubit represents the parity of multiple logical qubits. We show that the transformation renders diagonal multi-qubit operators between arbitrary logical qubits into single-qubit physical gates and, in turn, non-diagonal logical operators into sequences of physical gates. The transformation eliminates the need for long-range interactions and thus SWAP gates as illustrated in Fig. 1. Furthermore, redundant encoding provides intrinsic fault tolerance. We additionally present a possibility to choose and switch between different variants of the parity mapping, containing subsets of parity qubits tailored to the algorithmic requirements. This allows for further reduction of computational resources.

The gate set presented here contains operations that correspond to R_x and R_z rotations and controlled phase gates acting on logical qubits. Due to the absence of any connectivity limitations, we expect this approach to have an impact on the design of next generation

quantum devices [30]. The scheme allows for an efficient implementation of controlled rotations around the z -axis and is thus advantageous for the Quantum Fourier Transform [31] which is the basis of Shor’s factoring algorithm [22] as well as Quantum Addition [32]. Implementations of well known quantum algorithms in the parity architecture are shown in detail in the associated publication Ref. [33].

Parity Mapping The LHZ architecture [29] expands the Hilbert space of n logical qubits to a Hilbert space of $K = n(n - 1)/2$ physical qubits (parity qubits, with operators σ), encoding the parity of pairs of logical qubits (with operators $\tilde{\sigma}$) such that for any state $|\psi\rangle$ in the code space,

$$\tilde{\sigma}_z^{(i)} \tilde{\sigma}_z^{(j)} |\psi\rangle = \sigma_z^{(ij)} |\psi\rangle, \quad (1)$$

where the superscripts correspond to qubit labels. The code space is restricted to configurations corresponding to valid logical states $|\psi\rangle$ by $K - n + 1$ parity constraints of the form

$$C_l |\psi\rangle := \sigma_z^{(l_1)} \sigma_z^{(l_2)} \sigma_z^{(l_3)} [\sigma_z^{(l_4)}] |\psi\rangle = |\psi\rangle. \quad (2)$$

where the indices l_i correspond to pairs of logical indices, such that in every constraint, each logical index appears an even number of times. The brackets around $\sigma_z^{(l_4)}$ indicate that a constraint can contain either 3 or 4 qubits. Here, we use a slightly modified layout compared to the original LHZ layout, shown in Fig. 2, with an additional row of physical qubits which have a direct correspondence to single logical qubits,

$$\tilde{\sigma}_z^{(i)} = \sigma_z^{(i)}. \quad (3)$$

In the following, these additional qubits are referred to as *data qubits*. As depicted in Fig. 2, n all-to-all connected logical qubits are represented by $K = n(n + 1)/2$ physical qubits and $K - n$ constraints. The parity constraints generate the stabilizer of the code space [34], additionally allowing for detection of bit-flip errors and thus an intrinsic fault tolerance of the encoding.

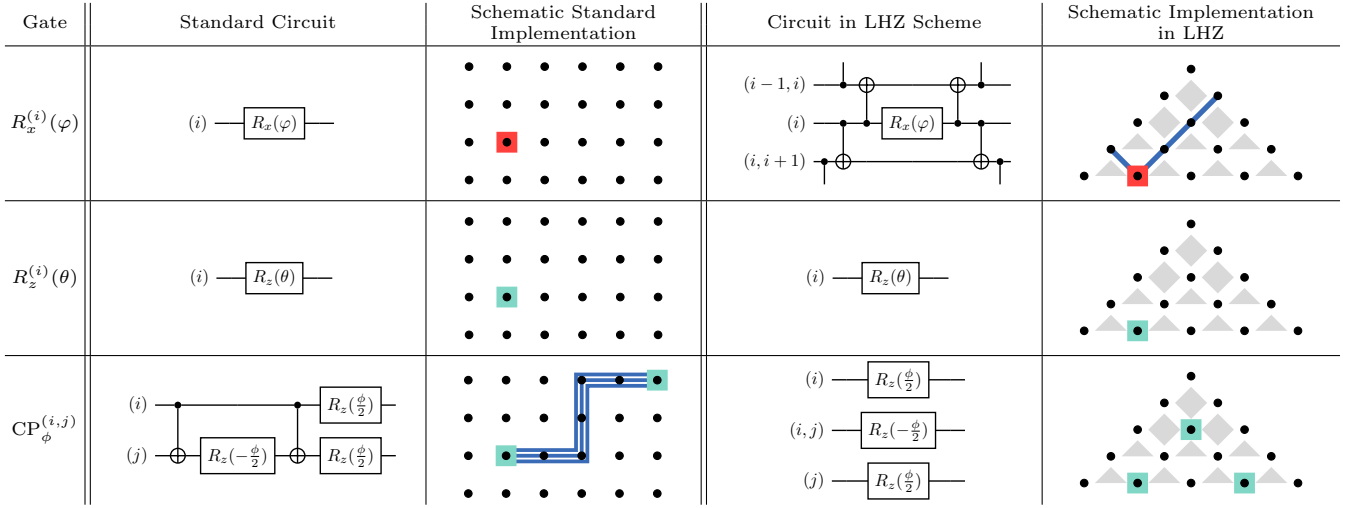


FIG. 1. Overview over the implementation of a universal gate set in the LHZ scheme. All operations have been decomposed to CNOT gates and local rotations. Blue lines represent a chain of CNOT gates, while red (darker) and green (lighter) squares depict local R_x and R_z rotations, respectively. Triple lines correspond to SWAP gates, consisting of 3 CNOT gates each.

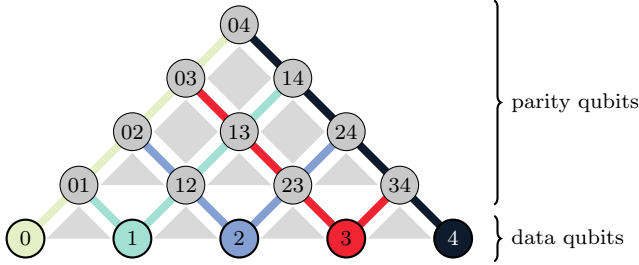


FIG. 2. Illustration of the modified LHZ architecture with logical lines. Three- and four-body constraints are represented by light gray triangles and squares between corresponding qubits. Data qubits with single logical indices are added as an additional row at the bottom of the architecture to allow direct access to logical R_z rotations. Colored lines connect all qubits whose labels contain the same logical index. Logical R_x rotations can be realized with chains of CNOT gates along the corresponding line.

Logical Qubits and Operators Next, we introduce the concept of *logical lines* denoted as Q_i , which have been identified in a different context in Ref. [35]. A logical line Q_i is defined as the set of all parity qubits containing the logical index i . In the LHZ architecture, qubits that contain a particular index are arranged along lines, which are indicated as solid lines in Fig. 2 to guide the eye. The red line for example extends from the data qubit (3) to all parity qubits that contain the index 3, and thus contain all relative parity information with respect to the logical qubit (3). For each logical line Q_i we define an operator

$$\tilde{\sigma}_x^{(i)} = \sigma_x^{(i)} \prod_{j < i} \sigma_x^{(ji)} \prod_{j > i} \sigma_x^{(ij)} \quad (4)$$

acting on every qubit in the respective line. The operators $\tilde{\sigma}_x^{(i)}$ and $\tilde{\sigma}_z^{(i)}$ commute with all parity constraints

and fulfill the (anti-) commutation relations for Pauli operators

$$\{\tilde{\sigma}_x^{(i)}, \tilde{\sigma}_z^{(i)}\} = [\tilde{\sigma}_x^{(i)}, \tilde{\sigma}_z^{(j)}] = 0 \quad (5)$$

for $i \neq j$. We can therefore identify the operators with Pauli operators acting on logical qubits, and build arbitrary logical rotations as

$$\tilde{R}_x(\alpha) = \exp\left(-i\frac{\alpha}{2}\tilde{\sigma}_x^{(i)}\right) \quad (6)$$

and

$$\tilde{R}_z(\alpha) = \exp\left(-i\frac{\alpha}{2}\tilde{\sigma}_z^{(i)}\right). \quad (7)$$

Throughout this work, tildes are used to denote operators with the corresponding action on logical qubits. While a logical \tilde{R}_z rotation can be directly implemented using the respective physical operator on the data qubit, the \tilde{R}_x operator on logical qubit (i) given by expression (6) can be implemented via physical CNOT gates along the logical line Q_i and a physical single-body R_x rotation, as depicted in Fig. 1 (also see Ref. [36] for details on efficient implementations of exponentials of multi-qubit Pauli operators). The chosen layout further ensures that all operators associated with the logical lines can be implemented with local operations and nearest-neighbor CNOT gates on a square lattice.

Encoding and Decoding In the following we discuss the encoding and decoding of arbitrary states from and to the data qubits. Let us first consider the trivial logical state $|0\rangle^{\otimes n}$ which can be encoded in the LHZ scheme by preparing all physical qubits in the product state $|0\rangle^{\otimes K}$. This state fulfills all constraints, and is the joint eigenstate of the logical $\tilde{\sigma}_z$ operators with eigenvalue

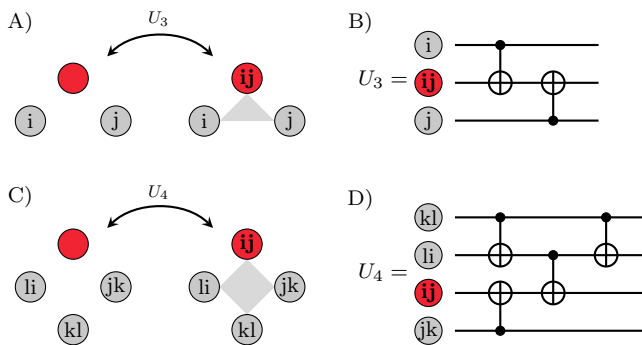


FIG. 3. Encoding and decoding circuits to add or remove a qubit and the corresponding constraint to or from the code. A) Qubit (ij) is directly encoded via the adjacent data qubits (i) and (j) in a three-body constraint, with the circuit B). C) Qubit (ij) is encoded using other parity qubits in a four-body constraint, with the circuit D). A qubit without label indicates a qubit without any parity information, being in the state $|0\rangle$.

+1. Encoding an arbitrary, unknown quantum state into the LHZ scheme is less straightforward. Classically, the states of the data qubits are identical to the corresponding logical qubits (by definition, a measurement of these qubits in the z -basis corresponds to a measurement of the logical state). However, they are typically highly entangled with the other qubits, and simply tracing out the parity qubits would cause a loss of coherence and therefore phase information.

We thus introduce an encoding and decoding strategy to add or remove an arbitrary number of parity qubits to or from the code. Suppose we start with the logical qubits, each of them encoded in a data qubit. We can now add a physical qubit (ij) corresponding to the parity of qubits (i) and (j) , by initializing this qubit in the state $|0\rangle$ and then imposing the parity on it with two CNOT gates controlled by qubits (i) and (j) , as shown in Fig. 3b. This procedure adds an additional parity qubit to the code and guarantees that the corresponding constraint $C = \sigma_z^{(i)} \sigma_z^{(j)} \sigma_z^{(ij)}$ is satisfied.

Following this procedure, it is possible to add parity qubits and constraints by applying this strategy iteratively. Instead of directly obtaining the parity information from the data qubits, one can also use the parity qubits included in local constraints, as for example the plaquettes shown in Fig. 2: By definition, the parity of all but one qubits of a constraint is always encoded in the state of the remaining qubit, i.e.

$$\begin{aligned} \sigma_z^{(ij)} \sigma_z^{(jk)} \sigma_z^{(kl)} \sigma_z^{(li)} |\psi\rangle &= |\psi\rangle \\ \Rightarrow \sigma_z^{(ij)} |\psi\rangle &= \sigma_z^{(jk)} \sigma_z^{(kl)} \sigma_z^{(li)} |\psi\rangle \end{aligned}$$

This transition and the encoding circuits are shown in Fig. 3c-d.

Conversely, applying the same gate sequence to a parity encoded set of qubits removes the targeted qubit from

the code and projects it to the state of the corresponding constraint. If the constraint was fulfilled, this is the state $|0\rangle$. For a layout as depicted in Fig. 2 with n logical qubits, this procedure allows encoding and decoding circuits with an overall circuit depth of $2n - 1$.

The described procedure does not only offer a way to build up or collapse the all-to-all connected LHZ scheme, but also holds the possibility to switch between different variants of the parity mapping and adapt the number of parity qubits to the algorithmic requirements during computation. For example, if some interactions are not needed for a certain algorithm, it is not always necessary to have the corresponding parity qubits in the code. A reduction in the number of parity qubits results in shorter logical lines and thus fewer physical gates. In addition to the two-body parities as introduced in Eq. (1), it is also possible to encode higher-order k -body parity qubits in the same manner, when using suitable layouts (see Ref. [33] for more detail). As an example, a three-body parity qubit can be used to enable a non-trivial interaction between three logical qubits.

Universal Gate Set Single-qubit operations on logical qubits can be constructed from the operators introduced in Eqs. (6-7) using the decomposition

$$U = R_z(\alpha) R_x(\beta) R_z(\gamma). \quad (8)$$

To obtain a universal gate set, an additional two-qubit entangling gate is necessary. In the LHZ encoding, a native logical two-qubit operation is obtained by performing a single R_z rotation on a physical parity qubit,

$$R_z^{(ij)}(\alpha) = \exp\left(-i\frac{\alpha}{2}\sigma_z^{(ij)}\right), \quad (9)$$

which is stabilizer-equivalent (i.e. the same up to application of a constraint operator $C = \sigma_z^{(i)} \sigma_z^{(j)} \sigma_z^{(ij)}$) to the operator

$$\exp\left(-i\frac{\alpha}{2}\sigma_z^{(i)} \sigma_z^{(j)}\right) \quad (10)$$

and thus effectively performs the two-body operation $\exp\left(-i\frac{\alpha}{2}\tilde{\sigma}_z^{(i)} \tilde{\sigma}_z^{(j)}\right)$ on the logical qubits, as obvious from Eq. (1). This operation can be transformed to a logical controlled phase gate CP_ϕ with local R_z rotations only, as shown in the following. For the sake of simplicity, qubit indices are omitted. We start from an operation

$$e^{-i\frac{\alpha}{2}\sigma_z \otimes \sigma_z} = \text{diag}\left(e^{-i\frac{\alpha}{2}}, e^{i\frac{\alpha}{2}}, e^{i\frac{\alpha}{2}}, e^{-i\frac{\alpha}{2}}\right) \quad (11)$$

and the single-body R_z rotation,

$$R_z(\theta) = e^{-i\frac{\theta}{2}\sigma_z} = \text{diag}\left(e^{-i\frac{\theta}{2}}, e^{i\frac{\theta}{2}}\right), \quad (12)$$

and define

$$U_R := [\mathbb{1} \otimes R_z(\beta)] e^{-i\frac{\alpha}{2}\sigma_z \otimes \sigma_z} [R_z(\gamma) \otimes \mathbb{1}]. \quad (13)$$

Evaluating Eq. (13) for $-\alpha = \beta = \gamma = \frac{\phi}{2}$, yields

$$U_R = e^{-i\frac{\phi}{4}} \cdot \text{diag}(1, 1, 1, e^{i\phi}) = e^{-i\frac{\phi}{4}} \cdot \text{CP}_\phi,$$

which corresponds, up to a global phase, to the controlled phase gate CP_ϕ . Using the identities defined above, this can be implemented in our scheme with local operations on the physical parity- and data qubits as

$$\text{CP}_\phi^{(i,j)} = R_z^{(i)} \left(\frac{\phi}{2} \right) R_z^{(ij)} \left(-\frac{\phi}{2} \right) R_z^{(j)} \left(\frac{\phi}{2} \right). \quad (14)$$

Here, i and j are the indices of the involved logical qubits and R_z indicates the rotation on the corresponding data or parity qubit. In particular, for $\phi = \pi$, we obtain the CZ gate (controlled-Z gate). This can in turn be transformed to a CNOT gate, by applying logical Hadamard gates before and after the CZ gate on the desired target qubit. The operations \tilde{R}_x , \tilde{R}_z and CP_ϕ form a *universal gate set* in the LHZ scheme and we can not only build arbitrary quantum circuits, but also exploit the comparably simple implementation of a controlled phase gate. The standard gate model requires 2 CNOT- and 3 single-qubit gates to implement a CPhase gate, as depicted in Fig. 1. Platforms with limited connectivity typically need a large number of SWAP gates in addition. In contrast, a logical CPhase gate in our approach only requires three parallel single-body rotations. The required resources for implementing common gates and gate sequences in our scheme are listed in Table I. The depth and the gate count for non-diagonal single-body operations result from the CNOT chains involved.

Following Eq. (8), any local unitary operation U on a logical qubit (i) can be performed in the LHZ scheme by performing it on the physical single-body qubit (i) and surrounding it by the CNOT-chains as in the logical \tilde{R}_x rotation,

$$\begin{aligned} \tilde{U} &= \underbrace{R_z^{(i)}(\alpha)}_{\tilde{R}_z} \dots \underbrace{\text{CNOT}^{(ij)} R_x^{(i)}(\beta) \text{CNOT}^{(ij)}}_{\tilde{R}_x} \dots \underbrace{R_z^{(i)}(\gamma)}_{\tilde{R}_z} \\ &= \dots \text{CNOT}^{(ij)} R_z^{(i)}(\alpha) R_x^{(i)}(\beta) R_z^{(i)}(\gamma) \text{CNOT}^{(ij)} \dots \\ &= \dots \text{CNOT}^{(ij)} U^{(i)} \text{CNOT}^{(ij)} \dots \end{aligned}$$

The circuit depth for this construction is given in Table I. Fixing the qubit on which the R_x rotations are performed to the respective data qubit reduces hardware requirements such that R_x rotations are only ever necessary on the data qubits, while for the parity qubits, local R_z rotations and CNOT gates between them are sufficient.

Note that a circuit implementing a product of $m \leq n$ logical single-qubit operators can be realized by applying the decoding circuit, performing the single-body operations on the data qubits and encoding again with an overall circuit depth of $4n - 1$ and a CNOT-gate count of $2n(n - 1)$. For a small number of simultaneous

| logic gate | required gates in LHZ | | |
|------------------------------|-----------------------|----------------------|--|
| | single-qubit | 2-qubit | depth |
| R_x | 1 | $2(n - 1)$ | $2 \lceil \frac{n}{2} \rceil + 1$ |
| σ_x | n | 0 | 1 |
| R_z | 1 | 0 | 1 |
| U | 3 | $2(n - 1)$ | $2 \lceil \frac{n}{2} \rceil + 1^a$ |
| CP | 3 | 0 | 1 |
| $\text{CNOT}^{(c,t)}$ | 7 | $2(n - 1 + c - t)$ | $\leq 4 \lceil \frac{n}{2} \rceil + 3^b$ |
| $\prod_{i=1}^m U_i^{(n_i)c}$ | $3m$ | $2m(n - 1)$ | $\leq 4n - 1$ |

^a For $n \leq 4$, the depth increases by two steps because the R_z rotations cannot be performed parallel to other operations.

^b Can be further optimized depending on the control- and target qubit. For a detailed discussion, see Ref. [33].

^c $n_i \leq n$ denotes the qubit on which U_i acts and $m \leq n$ is the number of qubits involved.

TABLE I. The number of physical operations needed to perform logical gates in the parity encoding for $n > 4$. All operations were decomposed into CNOT gates and local R_x and R_z rotations. The spin-flip operator σ_x is a special case of the R_x rotation, for which the logical implementation reduces to a product of single-qubit spin-flips which can be performed in parallel. The unitary U represents an arbitrary non-diagonal single-qubit operation. A detailed derivation of the given numbers can be found in Ref. [33].

single-qubit gates, a direct implementation without decoding can be advantageous as the required chains of CNOT gates can be partially parallelized.

Error Correction The redundancy of the parity encoding allows for error correction or mitigation. Because all parity constraints commute with any logical operator, measuring their value does not disturb the logical state of the system. Constraint measurements can be performed either with the help of ancillary measurement qubits in the center of each plaquette [31], or by applying the decoding circuit as in Fig. 3b/d to each constraint, measuring the decoded qubit, and encoding it again.

As the transition from one logical basis state to another flips n physical qubits, it is in principle possible to correct for multiple errors at a time. For example, F. Pastawski and J. Preskill successfully demonstrated error correction via belief propagation on an LHZ chip [37], and showed that the LHZ encoding is robust against weakly correlated bit-flip noise.

To ideally complement the bit-flip tolerance of the LHZ encoding, it is advisable to use physical qubits which are intrinsically robust against phase errors [38–40].

Conclusion and Outlook In conclusion, we have demonstrated a universal gate set implemented in the LHZ encoding, opening up a new strategy for universal quantum computation. All gates can be implemented on state-of-the-art quantum devices that fulfill the comparably low requirement of nearest-neighbor connectivity on a

square lattice. Furthermore, the encoding can be dynamically adjusted by adding or removing parity qubits tailored to the requirements of different algorithms. The introduced decoding scheme can be used to decode the output of optimization algorithms run in the parity scheme as for example proposed in Refs. [41–43], in order to further work with the resulting quantum states. With its availability of non-local and multi-qubit operations and the intrinsic error-correction capability, we expect our work to be a step towards the next generation of quantum computers.

Acknowledgements - Work at the University of Innsbruck is supported by the Austrian Science Fund (FWF) through a START grant under Project No. Y1067-N27 and the SFB BeyondC Project No. F7108-N38.

-
- [1] R. P. Feynman, Simulating physics with computers, *International Journal of Theoretical Physics* **21**, 467 (1982).
- [2] M. Reck, A. Zeilinger, H. J. Bernstein, and P. Bertani, Experimental realization of any discrete unitary operator, *Phys. Rev. Lett.* **73**, 58 (1994).
- [3] J. I. Cirac and P. Zoller, Quantum computations with cold trapped ions, *Phys. Rev. Lett.* **74**, 4091 (1995).
- [4] D. P. DiVincenzo, Two-bit gates are universal for quantum computation, *Phys. Rev. A* **51**, 1015 (1995).
- [5] A. Barenco, C. H. Bennett, R. Cleve, D. P. DiVincenzo, N. Margolus, P. Shor, T. Sleator, J. A. Smolin, and H. Weinfurter, Elementary gates for quantum computation, *Phys. Rev. A* **52**, 3457–3467 (1995).
- [6] S. Lloyd, Universal quantum simulators, *Science* **273**, 1073 (1996).
- [7] C. H. Bennett, E. Bernstein, G. Brassard, and U. Vazirani, Strengths and weaknesses of quantum computing, *SIAM Journal on Computing* **26**, 1510 (1997).
- [8] E. Knill, R. Laflamme, and W. H. Zurek, Resilient quantum computation: error models and thresholds, *Proc. R. Soc. Lond. A* **454**, 365 (1998).
- [9] D. Jaksch, J. I. Cirac, P. Zoller, S. L. Rolston, R. Côté, and M. D. Lukin, Fast quantum gates for neutral atoms, *Phys. Rev. Lett.* **85**, 2208 (2000).
- [10] R. Raussendorf and H. J. Briegel, A one-way quantum computer, *Phys. Rev. Lett.* **86**, 5188 (2001).
- [11] E. Knill, R. Laflamme, and G. J. Milburn, A scheme for efficient quantum computation with linear optics, *Nature* **409**, 46 (2001).
- [12] Y. Nakamura, Y. A. Pashkin, and J. S. Tsai, Coherent control of macroscopic quantum states in a single-cooper-pair box, *Nature* **398**, 786 (1999).
- [13] M. Saffman, T. G. Walker, and K. Mølmer, Quantum information with rydberg atoms, *Rev. Mod. Phys.* **82**, 2313 (2010).
- [14] K. Mølmer and A. Sørensen, Multiparticle entanglement of hot trapped ions, *Phys. Rev. Lett.* **82**, 1835 (1999).
- [15] A. Kitaev, A. Shen, M. Vyalıy, and M. Vyalıy, *Classical and Quantum Computation*, Graduate studies in mathematics, Vol. 47 (American Mathematical Society, USA, 2002).
- [16] J. Koch, T. M. Yu, J. Gambetta, A. A. Houck, D. I. Schuster, J. Majer, A. Blais, M. H. Devoret, S. M. Girvin, and R. J. Schoelkopf, Charge-insensitive qubit design derived from the cooper pair box, *Phys. Rev. A* **76**, 042319 (2007).
- [17] H. Häffner, C. F. Roos, and R. Blatt, Quantum computing with trapped ions, *Physics Reports* **469**, 155 (2008).
- [18] B. M. Terhal, Quantum error correction for quantum memories, *Rev. Mod. Phys.* **87**, 307 (2015).
- [19] D. Deutsch and R. Jozsa, Rapid solution of problems by quantum computation, *Proc. R. Soc. Lond.* **439**, 553 (1992).
- [20] A. Berthiaume and G. Brassard, Oracle quantum computing, *Journal of Modern Optics* **41**, 2521 (1994).
- [21] L. K. Grover, A fast quantum mechanical algorithm for database search, in *Proceedings of the Twenty-Eighth Annual ACM Symposium on Theory of Computing*, STOC '96 (Association for Computing Machinery, New York, NY, USA, 1996) p. 212–219.
- [22] P. W. Shor, Polynomial-time algorithms for prime factorization and discrete logarithms on a quantum computer, *SIAM Journal on Computing* **26**, 1484 (1997).
- [23] E. Bernstein and U. Vazirani, Quantum complexity theory, *SIAM Journal on Computing* **26**, 1411 (1997).
- [24] M. Mosca, *Quantum computer algorithms*, Ph.D. thesis, University of Oxford (1999).
- [25] G. Brassard, P. Høyer, M. Mosca, and A. Tapp, *Quantum amplitude amplification and estimation* (2002).
- [26] W. van Dam, Quantum algorithms for weighing matrices and quadratic residues, *Algorithmica* **34**, 413 (2002).
- [27] A. W. Harrow, A. Hassidim, and S. Lloyd, Quantum algorithm for linear systems of equations, *Phys. Rev. Lett.* **103**, 150502 (2009).
- [28] J. von Neumann, First draft of a report on the edvac, *IEEE Annals of the History of Computing* **15**, 27 (1993).
- [29] W. Lechner, P. Hauke, and P. Zoller, A quantum annealing architecture with all-to-all connectivity from local interactions, *Science Advances* **1**, e1500838 (2015).
- [30] J. Preskill, Quantum computing in the nisq era and beyond, *Quantum* **2**, 79 (2018).
- [31] M. A. Nielsen and I. L. Chuang, *Quantum Computation and Quantum Information: 10th Anniversary Edition*, 10th ed. (Cambridge University Press, USA, 2011).
- [32] T. G. Draper, *Addition on a quantum computer* (2000).
- [33] M. Fellner, A. Messinger, K. Ender, and W. Lechner, Applications of universal parity quantum computation, to be published (2022).
- [34] D. Gottesman, *Stabilizer codes and quantum error correction* (California Institute of Technology, 1997).
- [35] A. Rocchetto, S. C. Benjamin, and Y. Li, Stabilizers as a design tool for new forms of the lechner-hauke-zoller annealer, *Science advances* **2**, e1601246 (2016).
- [36] A. Cowtan, S. Dilkes, R. Duncan, W. Simmons, and S. Sivaram, Phase gadget synthesis for shallow circuits, *Electronic Proceedings in Theoretical Computer Science* **318**, 213–228 (2020).
- [37] F. Pastawski and J. Preskill, Error correction for encoded quantum annealing, *Phys. Rev. A* **93**, 052325 (2016).
- [38] P. Aliferis, F. Brito, D. P. DiVincenzo, J. Preskill, M. Steffen, and B. M. Terhal, Fault-tolerant computing with biased-noise superconducting qubits: a case study, *New Journal of Physics* **11**, 013061 (2009).
- [39] S. Puri, L. St-Jean, J. A. Gross, A. Grimm, N. E. Fratini, P. S. Iyer, A. Krishna, S. Touzard, L. Jiang, A. Blais,

- S. T. Flammia, and S. M. Girvin, Bias-preserving gates with stabilized cat qubits, [Science Advances](#) **6** (2020).
- [40] J. Lee, J. Park, and J. Heo, Rectangular surface code under biased noise, [Quantum Information Processing](#) **20**, 231 (2021).
- [41] W. Lechner, Quantum approximate optimization with parallelizable gates, [IEEE Transactions on Quantum Engineering](#) **1**, 1 (2020).
- [42] K. Ender, A. Messinger, M. Fellner, C. Daska, and W. Lechner, [Modular parity quantum approximate optimization](#) (2022).
- [43] L. M. Sieberer and W. Lechner, Programmable superpositions of ising configurations, [Phys. Rev. A](#) **97**, 052329 (2018).